



# Experimental and Theoretical Study on Electronic and Optical Properties of TiO<sub>2</sub> (anatase) Bulk and Al Doped Thin Film Phases

G. C. Kaphle<sup>1\*</sup>, R. P. Kharel<sup>2</sup> and B. P. Kafle<sup>3</sup>

<sup>1</sup>Central Department of physics, Tribhuvan University, Kirtipur, Kathmandu, Nepal

<sup>2</sup>Department of Physics, Tribhuvan University, Patan Multiple Campus, Lalitpur, Nepal

<sup>3</sup>Department of Chemical Science, Kathmandu University, Kavre, Nepal

\*corresponding Author: [gck223@gmail.com](mailto:gck223@gmail.com), [gopi.kaphle@cdp.tu.edu.np](mailto:gopi.kaphle@cdp.tu.edu.np)

Received: April 4, 2023

Revised: April 12, 2023

Accepted: June 28, 2023

## Abstract

Tuning the electronic and optical properties of TiO<sub>2</sub> is very important because of the variety of applications, including photocatalysts, electronics and data storage devices, and solar cells. Here, we performed the theoretical and experimental investigation of electronic, and optical properties of TiO<sub>2</sub> and Al doped TiO<sub>2</sub> in the form of bulk and thin film. A tight binding linear muffin-tin orbital (TB-LMTO) approach is used to optimize the TiO<sub>2</sub> (anatase) in bulk phase. The optimized lattice parameter of TiO<sub>2</sub> (anatase) is found to be 3.89 Å. The band structure plot reveals that bulk TiO<sub>2</sub> (anatase) bears wide bandgap semiconducting behavior with bandgap ( $E_g$ ) 3.23 eV whereas thin film of aluminium doped TiO<sub>2</sub> (anatase) behaves as a metal. The symmetric nature of up and down density of state (DOS) and projected density of states (PDOS) for both bulk and thin film of TiO<sub>2</sub> (anatase) ensures their non-magnetic behavior. Experimental observation shows that the surface reflectance of the film increases with increasing concentration of aluminium (Al) while transmittance observed as opposite trends. The direct and indirect bandgaps of TiO<sub>2</sub> film evaluated using transmittance curves are 3.53 eV and 3.27 eV respectively, which are well agreed with the available standard band-gap range of TiO<sub>2</sub> film (3.2 eV to 3.65 eV). The direct band gaps for Al-1% and Al-3% doped TiO<sub>2</sub> film are 3.60 eV and 3.62 eV respectively with thickness obtained from Swanepoel method are 682.06 nm and 745.56 nm respectively.

**Keywords:** TB-LMTO, Thin film, Spin coating, Bandgap, Swanepoel method

## 1. Introduction

TiO<sub>2</sub> is one of the frequently used materials material in a variety of products, including paints, varnishes, pigment, electrical ceramics, photo-catalysts, data storage and electronic devices [1-7]. TiO<sub>2</sub> primarily has three crystal structures: anatase (tetragonal, space group I4<sub>1</sub>/amd), rutile (tetragonal, space group P4<sub>2</sub>/mnm), and brookite (orthorhombic, space group Pbca) (Fig 1). Least stable structure of it named srilankite (called  $\alpha$ -PbO<sub>2</sub> type TiO<sub>2</sub> or TiO<sub>2</sub>-II) is also be found [8,9]. Out of them, rutile and anatase, are found in most stable states and hence both manufactured on an industrial scale. The rutile

phase begins to form above 600 °C whereas the anatase phase forms at lower temperatures [10]. TiO<sub>2</sub> nanoparticles typically develop an anatase phase rather than a rutile phase at a lower synthesis temperature (600 °C) because of the lower surface Gibbs free energy. The metastable brookite and anatase phases permanently change into the rutile phase while heated between 600 and 800°C [2]. Because of versatile application of inert and nontoxic TiO<sub>2</sub> in the fields of hydrogen production devices to medicine, and data storage devices to future generation technologies, we motivate to investigate pristine and doped properties in detail.

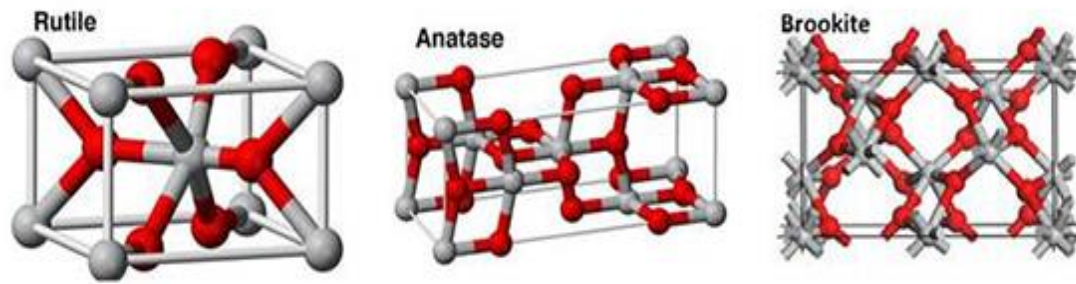


**Figure 1:** Unit cells of Rutile (Tetragonal), Anatase (Tetragonal) and Brookite (Orthorhombic) phase of  $\text{TiO}_2$ .

Titanium atoms are grey and, oxygen atoms are red (ref. 1)

$\text{TiO}_2$  actually has unpredictable electrical characteristics. If its average insulating qualities had to change to something more conducting or insulating, that would be intriguing. For it, we need to understand how electronic properties behaves and how doping affects them. This is the main motivation of present work.

Most of the electronic properties calculations show  $\text{TiO}_2$  has band gap ranging from (2.96eV- 3.35 eV) which is limited to application within UV regions [11]. The band gap properties increases and chemical properties changes due to quantum confinement effect. [12, 13, 14]. The Electronic properties of  $\text{TiO}_2$  can be tuned like other metal oxides [15,16,17]. It behaves more insulating after doping Ce and more conducting after doping Nb and Fe, respectively [18]. The electronic and optical properties of aluminium doped anatase and rutile  $\text{TiO}_2$  was performed by R. Shirely *et al.* In 2009 [1] using first-principles approach which could not define concentration dependent nature of band structure. The electronic structure and optical response of rutile, anatase and brookite  $\text{TiO}_2$  explore some intriguing properties [3]. Quantum-mechanical analysis of the equation of state of anatase  $\text{TiO}_2$  has also been discussed in 2001 by M. Calatayud *et al* [4]. Similarly, Humidity sensitive properties of nanostructured Al-doped  $\text{ZnO}:\text{TiO}_2$  thin films had performed by Weon-Pil Tai *et al.* in 2003 [5]. Enhanced efficiency of dye-sensitized  $\text{TiO}_2$  solar

cells (DSSC) by doping of metal ions is explained by K. H. Ko *et al.* [6]. The influence of film thickness on structural and optical properties of sol - gel spin coated  $\text{TiO}_2$  thin film [7] had also been studied. Each and every calculations and observations whatever explain including above mentioned literature show various conflicting and interesting results, though these properties are crucial for the practical applications. These results encourage us to go more insight into the pristine and doping properties.

The purpose of this paper is to investigate the influence of Al doping on the energetics, electronic structure and optical properties of anatase phases of pristine  $\text{TiO}_2$  theoretically and experimentally to explore the application of it in diverse area of physics.

## 2. Theoretical and Computational detail, and experimental procedure

### 2.1. Theoretical and computational details

Overall calculations were performed through the density functional theory implemented in Tight Binding Linear Muffin-Tin Orbitals Atomic Sphere Approximation (TB-LMTO-ASA) technique [19-21]. The exchange-correlation potential of Von Barth and Hedin is used for self consistency calculations to solve the Kohn-Sham equation with the aid of minimal basis sets and the partial wave approach as implemented within TB-LMTO-ASA code [22, 23]. For each atom in the unit cell, Wigner-Seitz spheres overlap to form the crystal potential which accounts

only the energetically higher-lying valence state for self-consistent computations. The local-density approximation (LDA) [5] as well as LSDA+U exchange correlation functional were used to get comparable structural and electronic properties with experiment. In this approximation, the deeper lying core states were treated as atomic like and hence called frozen core approximation. The band calculation technique are divided into two main approaches; one uses trial wave function, which is formed as linear combinations of basis functions like plane waves in the nearly free-electron (NFE) method expands orthogonalized plane waves function into a set of energy-dependent partial waves and applies a matching condition for partial waves at the muffin-tin sphere like the APW and KKR methods [24, 25(14)]. Actually, the linearized muffin-tin orbital (LMTO) method developed by Anderson [21, 22] uses as basis set for expanding the wave function, a set of orbitals that form a complete basis set for a muffin-tin potential.

For the computational calculation, every steps calculation of energy were iterated to self-consistency within the error bar less than  $10^{-6}$ Rydberg. Tetragonal nature of anatase phase of Titanium Dioxide having space group is  $I4_1/amd$  (space group number 141) with lattice parameter  $a = 3.785 \text{ \AA}$  and  $c = 9.514 \text{ \AA}$  was used. The position of Ti was taken as origin (0,0,0) and the position of O was used at (0,0,0.2064) [26]. For the doping purpose, the aluminium at different concentration was doped in interstitial region of pristine  $\text{TiO}_2$  (anatase). The geometrical optimization were fully optimized within LDA approach with force on each atom site less than  $0.05 \text{ eV/\AA}$ . The K grid mesh of  $4 \times 4 \times 3$  Monkhorst-Pack was used for geometry optimization, [15NN1] where as a  $10 \times 10 \times 8$  grid was used for electronic calculations.

In short, the LDA approach provides appropriate

geometry whereas incorrectly forecast the electronic properties of metal oxide like  $\text{TiO}_2$  [25]. To overcome such difficulty a Hubbard correction (DFT + U) is used which incorporates localised d and f electrons with a screened Coulomb interaction [27]. The value of U can be choosed in random manner otherwise has to be chosen through linear response approaches [28]. The value of U is system dependent and not transferable for the other systems under study.

## 2.2 Experimental procedure

Out of many technique [29], we employed spin coating technique for thin film preparation [30]. In order to make the titanium dioxide solution, 10 ml of ethanol and 1 ml of acetic acid were combined. After stirring it continuously for 15 minutes, 1.3 ml of titanium isopropoxide (TTIP) ( $\text{Ti} [\text{OCH} (\text{CH}_3)_2]_4$ ) was added drop by drop. Now, the mixture was bound with 2 drops of Triton X-100 and aged for 24 hours.

To make aluminium (Al) doped titanium dioxide solution, Titanium isopropoxide (TTIP) ( $\text{Ti} [\text{OCH}(\text{CH}_3)_2]_4$ ) was added drop by drop to 1.3 ml of ethanol and acetic acid, then the mixture was agitated for 15 minutes. Now, 0.03245g of  $\text{AgCl}_3$  (based on the atomic weight of Ti) was then added for 3% doping of aluminium, and it was agitated for 15 minutes. Triton X-100 was employed as a binder in 2 drops, which was also aged for 24 hours. Ordinary glass of thickness 0.1 cm used as micro slides for the deposition in the laboratories. At first the glass plate of dimension 1 cm x 1 cm x 0.1 cm was obtained using a diamond edge cutter, which was then washed through distilled water and ethanol then glass sample were cleaned using ultrasonic cleaner for about 5 minutes. The glass samples thus cleaned were dried at temperature  $100^\circ\text{C}$  and subjected to the deposition process. Cleaned and dried slides were placed at the coating spot in spin coater device. The spin coater

was fixed at 3000 rpm with time 30s to make homogeneous all over the substrate surface. 5 drop pure and aluminium doped  $\text{TiO}_2$  solution were poured on glass substrate by using syringe. After coating, coated slides were preheated at  $150^\circ\text{C}$  in high temperature closed muffle furnace for 10 min. This

process was repeated for six times to fabricate the pure and aluminium doped  $\text{TiO}_2$  thin film. Finally prepared film were annealed at  $450^\circ\text{C}$  in closed muffle furnace. Flow chart of thin film preparation of pure and Al doped  $\text{TiO}_2$  by spin coating is shown in figure (2).

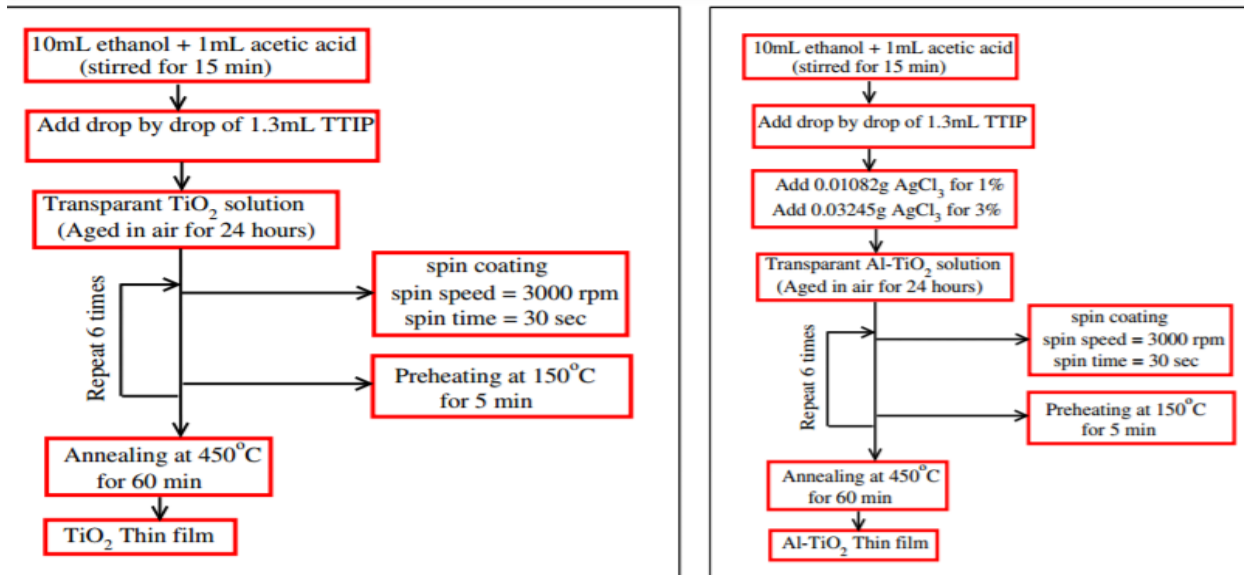


**Figure 2:** Mechanism involve in spin coating of pure (left) and aluminium doped (right) thin film of  $\text{TiO}_2$ .

Transmission and reflection were analysis using UV spectrometer (Thermo Scientific, UK, available in Kathmandu University) and a Reflectometric Spectrophotometer (Ang Tech., USA). The thickness ( $d$ ) and refractive index ( $n$ ) were estimated employing the well-known Swanepoel method [27]. The optical bandgap ( $E_g$ ) was estimated by the plot of  $(\alpha h\nu)^2$  vs  $h\nu$  for direct bandgap and  $(\alpha h\nu)^{1/2}$  vs  $h\nu$  for indirect bandgap [7], where  $\alpha$  is the absorption coefficient.

#### 4. Results and Discussion

This chapter summarizes the main findings from the TB-LMTO-ASA calculation for the structure and

electronic structure of Ti, pure  $\text{TiO}_2$  (anatase) and Al doped  $\text{TiO}_2$ . The results from the experimental contributions on optical properties of pure and Al doped  $\text{TiO}_2$  also summarized. The theoretical (TBLMTO-ASA) and experimental calculations are explained in short with discussion as follows,

#### 4.1 Theoretical (TBLMTO-ASA) calculations

##### 4.1.1 Structural analysis of pristine and Al doped $\text{TiO}_2$ (anatase)

$\text{TiO}_2$  (anatase) has a Tetragonal structure with the space group  $I4_1/amd$  having space group number 141.

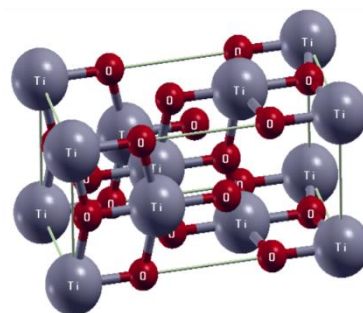
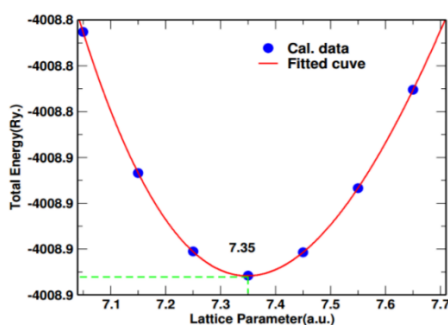


**Figure 3:** (a) Plot of energy vs lattice constant and (b) Optimized Crystal Structure of  $\text{TiO}_2$  (Anatase)

The lattice constant was taken to be  $a = b = 3.785 \text{ \AA}$  (7.155 atomic unit) and  $c = 9.514 \text{ \AA}$  (17.984 atomic unit) [26] as a base for optimized calculation. The structural optimization is performed through energy minimization process (Fig. 3a). The lattice constant for the optimized structure is obtained as  $3.888 \text{ \AA}$  (7.35 a. u.) close to experiment within the error-bar of

computational calculations. Further calculations are performed using this lattice constant. The energy minimization curve and optimized crystal structure are shown in figure (3).

Aluminium is doped in interstitial site without disturbing other parameter of pristine  $\text{TiO}_2$ (Anatase) as in figure.

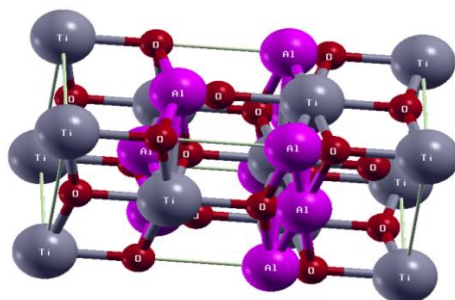


**Figure 4:** Unit cell Al doped  $\text{TiO}_2$  (anatase) in interstitial sites.

#### 4.1.2 Electronic properties of pristine and Al doped $\text{TiO}_2$ (anatase)

Using the optimized value of lattice constant ( $3.888 \text{ \AA}$ ), the band structure and density of states (DOS) of  $\text{TiO}_2$  (anatase) is determined within LDA along with Coulomb interaction parameter (LDA+U) approximation. As LDA underestimates the band gap of metal oxides, we have tested random value of U. The calculation shows that band gap properly opens

at  $U=7 \text{ eV}$  with band gap  $3.23 \text{ eV}$  close to the experimental [31] (**Fig. 5 a, 5b**). Figure (5) shows that the indirect band gap is observed at  $X-\Gamma$  with band gap  $3.23 \text{ eV}$ . We observed 38 bands within the energy range of  $52.87 \text{ eV}$  ( $\Gamma_{\text{Max}}= 35.81 \text{ eV}$   $\Gamma_{\text{Min}}=-17.06 \text{ eV}$ ). The band gaps at different symmetric points under LDA and LDA+U along with experimental value is depicted in table (1).

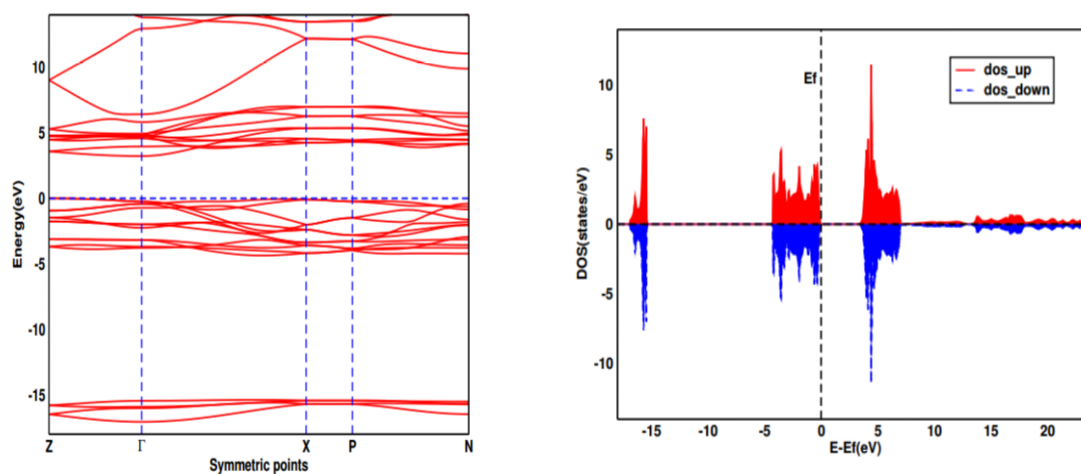


**Figure 5:**(a) Band structure and (b) DOS of  $\text{TiO}_2$ (anatase) under LDA+U ( $U = 7 \text{ eV}$ ) approximation.

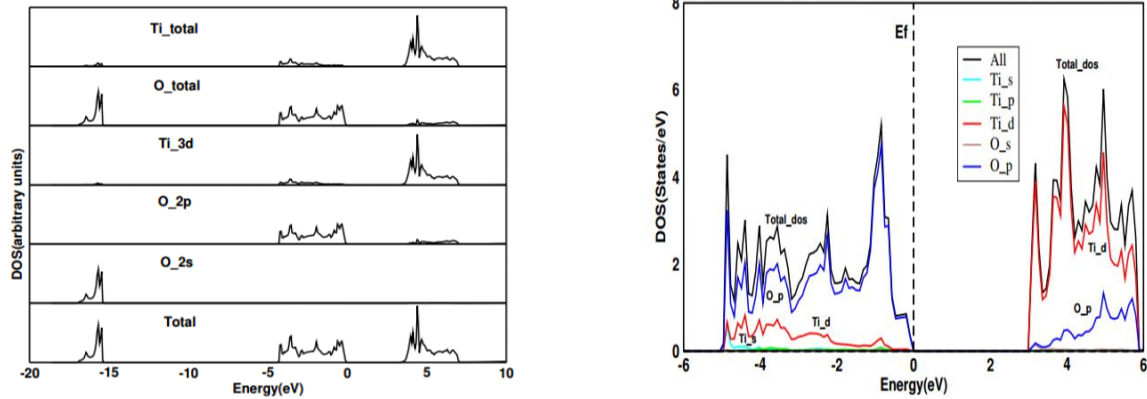
**Table 1:** Band gap of TiO<sub>2</sub> (anatase) at different symmetrical points under LDA and LDA+U approximation along with experimental result.

Symmetric Points	LDA (eV)	LDA + U(eV)	Exp.(eV)
X- $\Gamma$	1.98	3.23	3.20 [31]
$\Gamma$ - $\Gamma$	2.14	3.49	
X-Z	2.28	3.59	
X-X	3.10	4.24	
X-P	3.30	4.31	
X-N	3.00	4.12	

The band structure and symmetric nature of up and down Density of States (DOS) calculations reveal that TiO<sub>2</sub> at anatase phase behaves as wide band gap semiconductor with para-magnetic behavior.

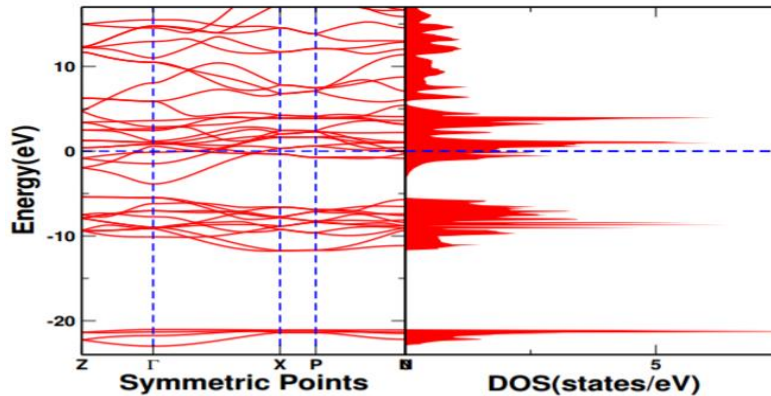
The contributions of different orbitals of Ti and O are

obtained from projected DOS (Fig. 6). From the figure, it is seen that the valance band edge of TiO<sub>2</sub> (anatase) is dominated by O-2p, and the conduction band edge is formed from Ti-3d.

**Figure 6:** PDOS of TiO<sub>2</sub> under LDA+U with U=7eV approximation.

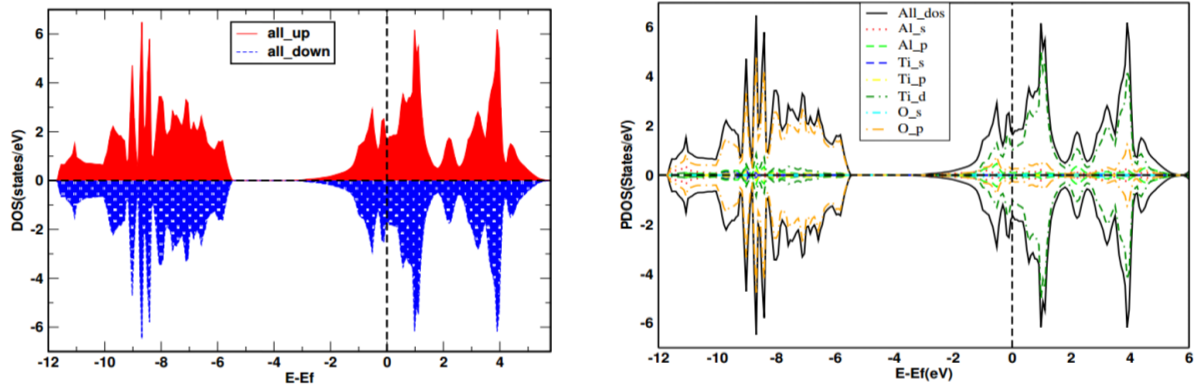
Now for the doping procedure, we have chosen interstitial sites so that there is no change in band number and lattice parameters. After doping

TiO<sub>2</sub> anatase, its semiconducting nature changes to conducting (Fig.7)

**Figure 7:** Band structure along with total DOS of Al doped TiO<sub>2</sub>.

At the same time the energy range so obtained bands are squeezing to 51.58 eV ( $\Gamma_{\text{Max}}= 28.41$  eV  $\Gamma_{\text{Min}}=-23.17$  eV) indicating that bands are closely compact. After adding aluminium in empty sphere, the distance between the atoms become shorter as a results of it bands are shifted downward the Fermi level and

hence overlapping of conduction and valance bands give rise to metallic behavior. The symmetric nature of up and down spins of total DOS and PDOS indicating that Al-doped systems is non- magnetic conducting material (Fig. 8a,b).



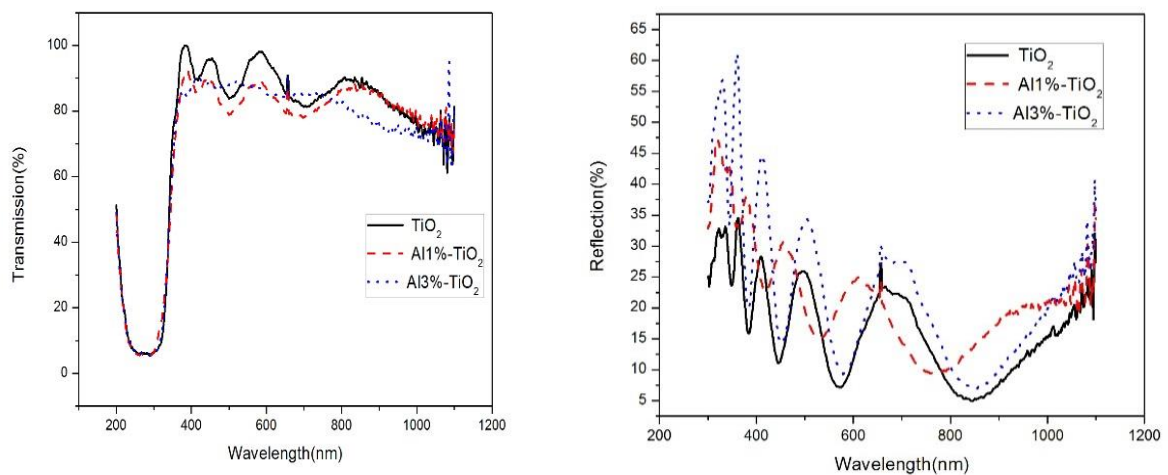
**Figure 8:** (a) Total DOS and (b) PDOS of Al - TiO<sub>2</sub> under LDA approximation. The vertical dotted line represent the Fermi level.

Figure 8 shows that in the Fermi level of Al-TiO<sub>2</sub> valance and conduction band edges are dominated by Ti-d and O-p and presence of other orbital are very minimum comparison to Ti-d and O-p.

#### 4.2 Experimental measurements

The TiO<sub>2</sub> thin films transmittance were measured using UV visible spectrophotometry, over the range 200 nm - 1100 nm. The transmittance spectra were

recorded at 2 nm wavelength interval at room temperature. The optical transmittance spectra of TiO<sub>2</sub> in figure (9a) were derived by averaging of 5 measurements (at 5 locations, center and 4 other location around center). The spectra apparently show that at  $\lambda$  above 400 nm the films are highly transparent up to max. 90 % with average value of 85 %. While, transparency show gradual decreases with increase of wavelength as shown in figure (10 b).



**Figure 9:** (a) Optical transmission and (b) reflection spectra of pristine and Al doped TiO<sub>2</sub> thin film.

It is also seen that in the wavelength range of 200 nm - 350 nm, the transmittance of thin film has reduced to minimum value up to 4 - 5%, indicating the opacity to UV in the range 200 nm - 350 nm due to absorption of UV radiation by TiO<sub>2</sub> crystals.

Surface reflectance of above indicated films were also recorded and presented in the figure (10b).

**Table 2:** Optical values of pristine and Al doped TiO<sub>2</sub> thin film by spin coating method.

Sample	Undoped TiO <sub>2</sub>	Al-1% TiO <sub>2</sub>	Al-3% TiO <sub>2</sub>
Transmittance (%)	74.3	71.5	70.7
Reflectance (%)	16.5	21.4	22.6
Thickness (nm)	491.52	682.06	745.56
Direct bandgap (eV)	3.53	3.60	3.62
Indirect bandgap (eV)	3.27		
Theoretical indirect bandgap (eV) (present)	3.23		
Experimental bandgap (eV) (previous)	3.20 [31]		

Table (2) also listed the thickness for pure and Al doped TiO<sub>2</sub> thin film, which were extracted from the well-known Swanepoel method [32]. That is the thickness of the film using this method can be calculated using the equation

$$d = \frac{\lambda_1 \lambda_2}{2(\lambda_1 n_2 - \lambda_2 n_1)}$$

Where,  $n_1$  and  $n_2$  are the refractive indices calculated from two consecutive maxima or minima corresponds to two wavelengths of  $\lambda_1$  and  $\lambda_2$ . Table 2 shows that the thickness of film is increased with increasing aluminium concentrations.

The band gap of thin films can be determined from:

$$\alpha h\nu = A(h\nu - E_g)^r$$

Where A is a constant,  $h\nu$  is the photon energy,  $E_g$  is the optical energy gap of the material, and the exponent r, is characteristic of the type of the optical transition process [33]. The value of r takes as 1/2, 3/2, 2 and 3 for direct allowed, direct forbidden,

Similar to method adopted for transmittance measurement, the reflectance shown in figure (10b) are produced by averaging 5 measurement for each samples. It is observed that increasing trend reflectance is appeared with increasing Al concentration which is tabulated in Table (2).

indirect allowed and indirect forbidden transitions respectively [7]. The slope of plot  $(\alpha h\nu)^2$  and  $(\alpha h\nu)^{1/2}$  along Y-axis and  $h\nu$  in along X-axis gives direct and indirect band gap. From the experimental (slope) study the direct and indirect band gap ( $E_g$ ) found as 3.53 eV and 3.27 eV for TiO<sub>2</sub> respectively which is comparable to theoretical result. Similarly Al-1% doped and Al-3% doped TiO<sub>2</sub> thin film show direct types of band gaps with values 3.60 eV and 3.62 eV respectively. These results also supports the quantum confinement assumption. The band gaps of Aluminium doped TiO<sub>2</sub> is slightly increased with the increase of concentration of aluminium p is depicted in table (2). The slightly larger optical band gap (3.27 eV) energy than the reported value for bulk anatase (3.2 eV) is due to the lattice distortion produced by a mismatch between the film and the substrate [33,34].



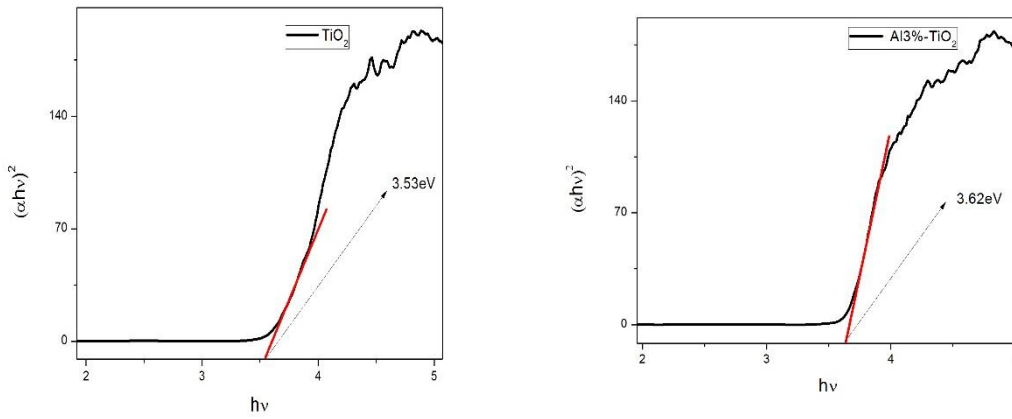


**Figure 10:** The direct (left) and indirect (right) bandgap for pristine  $\text{TiO}_2$  from the experiment.

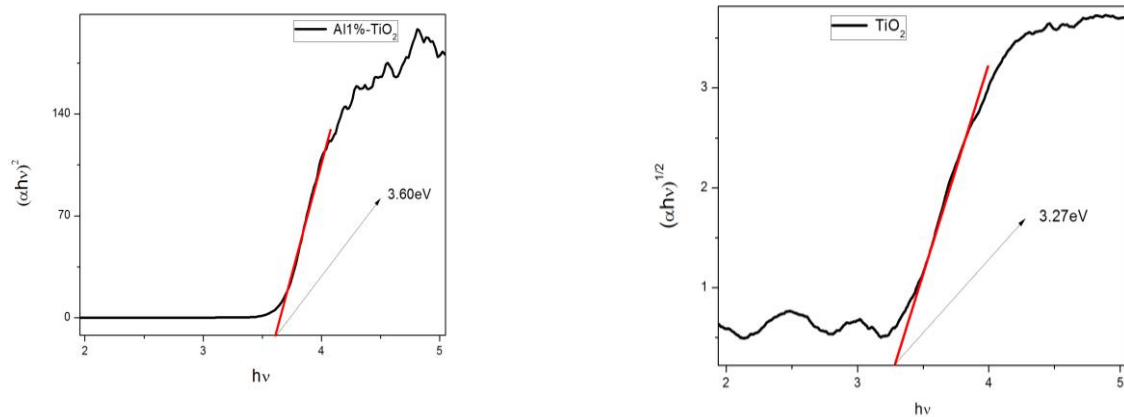


**Figure 11:** The estimated band gaps for Al-1% doped  $\text{TiO}_2$  (left) and Al-3% doped  $\text{TiO}_2$  (right) obtained from experiment.

## 5. Conclusions

Present result compared the experimental and theoretical calculations. The optimized lattice parameter obtained from first principle approach for pristine  $\text{TiO}_2$  3.888 Å with c/a ratio 2.5, which is comparable to experiment as well as previously reported data indicating that we have successfully prepared porous and transparent  $\text{TiO}_2$  thin films using titanium isopropoxide. The indirect band gap of pristine  $\text{TiO}_2$  (Anatase) from DFT +U calculations through TB-LMTO approach is found 3.23 eV with  $U=7\text{eV}$ , which is close to experimental result 3.27 eV. The slight discrepancy is mainly due to the lattice distortion produced by a mismatch between the film and the substrate. The optical properties of  $\text{TiO}_2$  were investigated using Spectroscopic refractometer, The

thickness of the six cycle coated thin film of pure  $\text{TiO}_2$  was found to be 491.52 nm and band gap value was to be 3.27 eV (indirect) and 3.53 eV (direct). When aluminium is doped at interstitial region of  $\text{TiO}_2$ , the valance bands and conduction bands are found to be overlapping with each other indicating metallic nature. The symmetric nature of up and down DOS and PDOS of  $\text{TiO}_2$  (anatase) and Al doped  $\text{TiO}_2$  show that both pristine and doped systems are non-magnetic in nature. As concentration of Al doped on the thin film of pristine  $\text{TiO}_2$  increased slightly 1% Al doped (3.60 eV) and 3% Al doped  $\text{TiO}_2$  (3.62 eV), band gap also increased, respectively, which also follows the quantum confinement properties. While Al is substituted in the interstitial sites without changing bands number and volume system becomes conductor.

## References

- [1] R. Shirley, O. R. Inderwild, M. Kraft, Electronic and Optical properties of aluminium doped anatase and rutile TiO<sub>2</sub> from abinitio calculations. University of Cambridge, UK (2009).
- [2] N. N. Greenwood, A. Earnshaw, Chemistry of the Elements. Oxford: Pergamon Press. pp. 1117, ISBN 0-08-022057-06, USA (1984).
- [3] M. Landmann, E. Rauls and W. G. Schmidt. The electronic structure and optical response of rutile, anatase and brookite TiO<sub>2</sub>. *J. Phys. Condens. Matter*, **24**, 195503, (2012).
- [4] M. Calatayud, P. Mori-Sanchez, A. Beltran, A. M. Pendas, E. Francisco, J. Andres and J. M. Recio. Quantum-mechanical analysis of the equation of state of anatase TiO<sub>2</sub>. *Phys. Rev. B*, **64**, 184113, (2001).
- [5] W. P. Tai, J. G. Kim, J. H. Oh. Humidity sensitive properties of nanostructured Al-doped ZnO: TiO<sub>2</sub> thin films. *Sensors and Actuators B* **96**, 477, (2003).
- [6] K. H. Ko, Y. C. Lee, Y. J. Jung. Enhanced efficiency of dye-sensitized TiO<sub>2</sub> solar cells (DSSC) by doping of metal ions. Department of Materials Science and Engineering, Ajou University, Suwon 442-749, South Korea, (2004).
- [7] P. Malliga, J. Pandiarajan, N. Prithivikumaran and K. Neyvasagam. Influence of Film Thickness on Structural and Optical Properties of Sol Gel Spin Coated TiO<sub>2</sub> Thin Film. *J. Appl. Phys.*, **6**(1), 22-28, (2014).
- [8] R. W. G. Wyckoff: "Crystal structure", Interscience Publishers, New York (1965).
- [9] J. Haines and J. M. Léger, "X-ray diffraction study of TiO<sub>2</sub> up to 49 Gpa" *Physica B* **192**, 233(1993).
- [10] A. J. Haider, J. N. Jameel, I. H.M. Al-Hushain, "Review On: Titanium Dioxide Applications, Energy Procedia", **157**, 17-29 (2019).
- [11] S. O. Kasap, "Principles of Electronic Materials and Devices "Second edition , McGraw Hill, Newyork 557 (2002).
- [12] T. Seiyama, A. Kato, K. Fujisishi and M. Nagatoni, "A new detector for gaseous components using semiconductive thin films", *Analytical Chemistry*, **34**, 1052(1992).
- [13] K. I. Gnanasekar and B. Rambabu "Nanostructure semiconductor oxide powders and thin films for gas sensor ", *Surface Science*, **200**, 780(2002).
- [14] S. Datta, G. C. Kaphle, S. Baral, A. Mookerjee, Study of morphology effects on magnetic interactions and band gap variations for 3d late transition metal bi-doped ZnO nanostructures by hybrid DFT calculation, *J. Chem. Phys.* **143**, 084309 (2015) .
- [15] G. R. Haripriya *et al.*. Spin reorientation in antiferromagnetic Dy<sub>2</sub>FeCoO<sub>6</sub> double perovskite, *J. Phys.: Condens. Matter* **33**, 025802(2021).
- [16] T. P., Yadav, A. Srivastava, & G. C. Kaphle, Magnetism in Zigzag and Armchair CuO Nanoribbons: Ab Initio Analysis. *Phys. Solid State* **63**, 279–285 (2021).
- [17] J. W. Pan, C. Li, Y. F. Zhao, R. X. Liu, Y. Y. Gong, L. Y. Niu, X. J. Liu, B. Q. Chi, Electronic properties of TiO<sub>2</sub> doped with Sc, Y, La, Zr, Hf, V, Nb and Ta, *Chemical Physics Letters*, **628**, 43-48 (2015).
- [18] D. Mardare, G. I. Rusu, COMPARISON OF THE DIELECTRIC PROPERTIES FOR DOPED AND UNDOPED TiO<sub>2</sub> THIN FILMS, *J. Optoelec. Adv. Matt.*, **6**(1), 333 - 336 (2004).
- [19] W. Kohn, and L. J. Sham. Self-consistent equations including exchange and correlation effects. *Phys. Rev.* **140**, A1133 (1965).
- [20] M. Dreizler, Reiner, and E. K. Gross. Density Functional Theory: An Approach to the Quantum Many-Body Problem, Springer, New York

- (1990).
- [21] C. M. Fang, G. A. de Wijis, R. A. de Groot. Spin-polarization in half-metals, *J. Appl. Phys.***91**, 8340-8344, (2002).
- [22] N. W. Ashcroft and N. D. Mermin. *Solid state Physics*. Saunders College Publishing, USA (1976).
- [23] H. L. Skriver. *The LMTO Method Muffin Tin Orbital and Electronic Structure*, **41**, Springer-verlag, Berlin Heidelberg(1984).
- [24] U. Mizutani. *The Electronic Theory of Metals*, 1st edition, Cambridge University Press. New York (1984).
- [25] O. K. Andersen, O. Jepsen and G. Krier. *Lecture Notes on methods of Electronic calculations*, ed. V. Kumar, O. K. Andersen, and A. Mookerjee, World Scientific Publ. Co., Singapore (1994).
- [26] Y. Xu, E. M. Lotfabad, H. Wang, B. Farbod, Z. Xu, A. Kohandehghan and D. Mitlin. *Nanocrystalline Anatase TiO<sub>2</sub>: a New Anode Material for Rechargeable Sodium Ion Batteries*, Department of Chemical and Materials Engineering, University of Alberta, 9107-116 St., Edmonton, AB, Canada T6G 2V4. (2013).
- [27] Baoshun Liu, Xiujian Zhao, The synergetic effect of V and Fe-co-doping in TiO<sub>2</sub> studied from the DFT+U first-principle calculation, *Appl. Surf. Sci.*, **399**, 654-662(2017).
- [28] Monkhorst, H. J.; Pack, J. D., Special points for Brillouin-zone integrations. *Phys. Rev. B*, **13**, 5188-5192 (1976).
- [29] Doubi, Y., Hartiti, B., Labrim, H. *et al.* Experimental study of properties of TiO<sub>2</sub> thin films deposited by spray pyrolysis for future sensory applications. *Appl. Phys. A* **127**, 475 (2021).
- [30] M. D. Tyona, A comprehensive study of spin coating as a thin film deposition technique and spin coating equipment, *Advances in Material Research*, **2**( 4) 181-193 (2013) .
- [31] H. Tang, K. Prasad, R. Sanjinbs, P. E. Schmid, and F. Levy, Electrical and optical properties of TiO<sub>2</sub>anatase thin films, *J. Appl. Phys.***75**, 2042–2047 (1994)
- [32]Dorrnian, D., Dejam, L. & Mosayebian, G. Optical characterization of Cu<sub>3</sub>N thin film with Swanepoel method. *J. Theor. Appl. Phys.***6**, 13 (2012).
- [33] J. K. Shang, P. G. Wu and C. H. Ma. Effects of nitrogen doping on optical properties of TiO<sub>2</sub> thin films. *Applied Physics*, **81**(1), 1411 (2005).
- [34] J. Cao and J. Wu, Strain effects in low-dimensional transition metal oxides. *Materials Science and Engineering R* **71**, 35-52 (2011).